

# Endothelial Nitric Oxide Deficiency Reduces MMP-13–Mediated Cleavage of ICAM-1 in Vascular Endothelium

## A Role in Atherosclerosis

Carlos Tarín, Monica Gomez, Enrique Calvo, Juan Antonio López, Carlos Zaragoza

**Objective**—Lack of endothelial nitric oxide synthase worsens atherosclerosis at least by increasing monocyte adhesion to endothelial cells. The purpose of this study was to elucidate the molecular mechanism elicited by NO.

**Methods and Results**—We evaluated atherosclerosis in apoE and NOS3/apoE-deficient mice fed with high-cholesterol diet. We found significant increase in aortic lesion size, and infiltration of macrophages in NOS3/apoE-null mice when compared to apoE-deficient animals. To test the relevance of cellular adhesion as well as extracellular matrix degradation, we evaluated ICAM-1, VCAM-1, PECAM-1, MMP-2, MMP-9, MMP-12, MT1-MMP, and MMP-13 levels in mouse aortas. Lack of NO inhibits MMP-13 and increases ICAM-1 levels in atherosclerosis as compared to apoE-null mice. Ectopically expression of ICAM-1 in eukaryotic cells revealed that extracellular domain of ICAM-1 harbors a substrate recognized by MMP-13. Incubation of COS-7 cells expressing ectopic ICAM-1 in the presence of active MMP-13 induced inhibition of RAW 264.7 cell adhesion to COS-7 monolayers. MALDI-TOF MS analysis combined to Liquid chromatography coupled to Ion Trap MS on ICAM-1 incubated with MMP-13 allowed us to determine the cleavage sites of MMP-13 at positions E61 and G98 of ICAM-1. G98 is part of a PDGQS moiety, which shows homology with the consensus PDGLS substrate located at the MMP-13 cleaved site of type II collagen I-alpha.

**Conclusions**—Taking together, these results point toward MMP-13 as a mechanism for the NO-mediated protection of atherosclerosis. (*Arterioscler Thromb Vasc Biol.* 2009;29:27-32.)

**Key Words:** atherosclerosis ■ nitric oxide ■ NOS3/apoE-null mice ■ MMP-13 ■ ICAM-1

During atherosclerosis attachment of circulating mononuclear cells to the vessel wall<sup>1</sup> is mediated by adhesion molecules, including vascular cell adhesion molecule 1 (VCAM-1), platelet cell adhesion molecule 1 (PECAM-1), and intracellular cell adhesion molecule 1 (ICAM-1). In aortas of apoE-null mice, ICAM-1 was found located in lesion-prone sites of the aorta,<sup>2</sup> and the importance of this inflammatory molecule was evidenced in atherosclerotic mice deficient in ICAM-1, which resulted protected from atherosclerotic lesions.<sup>3</sup>

The role of matrix metalloproteinases (MMPs) has been analyzed in detail in late atherosclerosis.<sup>4,5</sup> However, the precise role of MMPs in the early steps of this pathology is still debated. In this regard, the effect of MMPs in the shedding of adhesion molecules was investigated in vitro,<sup>6</sup> although no data were reported in the context of atherosclerosis.

Lack of endothelial NOS (eNOS, NOS3) increases leukocyte-endothelial adhesion, smooth muscle cell migration, platelet aggregation, and atherosclerosis in mice.<sup>7,8</sup> However, the mechanisms by which NOS3 could prevent atherosclerosis still remain unclear. Here we found that in

atherosclerotic NOS3/apoE-deficient mice, increased monocyte adhesion, and a significant reduction of MMP-13 expression, were detected when compared to apoE-deficient animals. In addition, we found that MMP-13 cleaves ICAM-1 both in vivo and in vitro. Mass spectrometry analysis revealed 2 sites at positions E61 and G98, close to the ICAM-1 extracellular N-terminal domain. The relevance of MMP-13 and ICAM-1 on cellular adhesion was found in COS-7 cells expressing ectopic ICAM-1, in which RAW 264.7 cell adhesion was inhibited by the presence of active MMP-13. Our findings may help to explain at the molecular level the protective effect of endothelial NO in atherosclerosis.

## Methods

### Reagents

General cell culture supplies were from BD Biosciences, calf serum was from BioWhittaker, and cell culture gelatin, antibiotics, and Oil Red were from Sigma. Autoradiography film was from Kodak; polyvinylidene fluoride (PVDF) protein transfer membranes from Millipore; and HRP-conjugated secondary antibodies, the ECL immunoblot detection system, and protein-A/G-sepharose were from GE HealthCare. EDTA-free protease inhibitor cocktail tablets were

Received May 3, 2008; revision accepted October 20, 2008.

From the Fundación Centro Nacional de Investigaciones Cardiovasculares (CNIC), Melchor Fernández Almagro 3, 28029 Madrid, Spain.

Correspondence to Carlos Zaragoza, Fundación CNIC, Melchor Fernández Almagro 3, 28029 Madrid, Spain. E-mail czaragoza@cnic.es

© 2008 American Heart Association, Inc.

*Arterioscler Thromb Vasc Biol* is available at <http://atvb.ahajournals.org>

DOI: 10.1161/ATVBAHA.108.169623

from Roche. Optimem and Lipofectamine were from GIBCO. Membrane-permeant reactive cell tracker CMT-MR was from Invitrogen. Anti-MMP-2, anti-MMP-9, anti-MMP-13, and Fluorsave cover slip mounting solution were obtained from Calbiochem; Anti-6XHis antibody was from Sigma. Anti-GAPDH, anti-ICAM-2, and anti-VWF were from BD Biosciences, Anti-MOMA-2 antibody was from Serotec.

### Animals and Diet

Wild-type C57BL/6 mice, NOS3-null mice, and apoE-null mice were purchased from The Jackson Laboratory. NOS3/apoE-double null mice were generated in our animal facility. Atherosclerosis was induced in mice fed with Western diet for 16 weeks (42% fat, Harland Teklad, TD88137). All animals were housed in isolated rooms.

The investigation conforms to the Guide for the Care and Use of Laboratory Animals published by the US National Institutes of Health (NIH Publication No. 85-23, revised 1996).

### Cells

COS-7 cells were grown as previously described.<sup>9</sup>

### Plasmids and Cell Transfection

Epitope-tagged construct encoding full-length ICAM-1 was generated by Dra Olga Barreiro<sup>10</sup> and kindly donated by Prof Francisco Sánchez-Madrid, and expressed in COS-7 cells as indicated (Servicio de Inmunología, Hospital de la Princesa, Universidad Autónoma de Madrid, Spain). Cells were transiently transfected using Lipofectamine 2000 Reagent as previously described.<sup>9</sup> Expression was monitored by confocal immunofluorescence microscopy and immunoblotting with the corresponding antibodies.

### Flow Cytometry Assay

Surface expression of macrophage markers and GFP-fluorescence were determined by flow cytometry using a CyAn MLE flow cytometer (DakoCytometry). Aortas or cells were homogenized in a PBS trypsin/EDTA-containing buffer. For GFP detection, cells were rinsed in PBS and subjected to flow cytometry. For macrophage detection, blood or homogenated tissue was incubated with anti-MOMA-2 for 1 hour at 4°C. After cells were rinsed 3 times with ice-cold PBS, they were incubated with a secondary antibody coupled to fluorescein isothiocyanate (FITC). After wash in PBS, cells were analyzed.

### Quantitation of Lesion

Mice were euthanized and entire aortas were isolated from the heart to the iliac bifurcation, cut open longitudinally, and stained with Oil Red O reagent. Aortas were washed 3 times to remove excess of staining solution, photographed, and lesions counted. In addition, ascending aortas were isolated and eosin-hematoxylin stained. Representative photomicrographs were taken from each sample, and area plaques were calculated using Image J software.

### Confocal Microscopy

Mice were anesthetized, and thoracic aortas were harvested. Samples were embedded in paraffin, and 4-mm-thick serial sections were subjected to eosin-hematoxylin staining, confocal microscopy, or immunohistochemistry with the appropriated antibodies as described.<sup>11</sup>

### Cell Adhesion Assay

To quantify monocyte adhesion to COS-7 cell monolayers, RAW cells were incubated 15 minutes at 37°C in the presence of the fluorescent probe CMT-MR. Cells were then centrifuged at 1400 rpm for 5 minutes, and then resuspended in HBSS +1% BSA. 10<sup>6</sup> labeled RAW cells per well were placed on COS-7 monolayers transiently transfected or not with a plasmid encoding ICAM-1, and incubated for 30 minutes at 37°C, in the presence or absence of 1 μg MMP-13. Wells were filled with HBSS +0.1% BSA, sealed with

adhesive plastic seal, and kept on inverted position for 20 minutes. Buffer was then removed, and cells were lysed in 0.1% SDS, 50 mmol/L Tris, pH 8.5. Fluorescence was measured in a microplate reader (excitation wavelength: 544 nm; emission wavelength: 590 nm).

### Analysis of MMP-13 Cleavage by Mass Spectrometry

Samples containing either ICAM-1, MMP-13, or both molecules were digested by adding 0.5 mg modified porcine trypsin (sequencing grade, Promega) per sample. The resulting tryptic peptides were first analyzed by MALDI-TOF MS (Ultraflex TOF/TOF, Bruker Daltonics). A volume of 0.5 μL of 2,5-Dihydroxybenzoic Acid (DHB) matrix (0.3 g/L) was mixed with 0.5 μL of each digested sample onto an AnchorChip MALDI plate (Bruker Daltonics). Mixtures were let to dry to room temperature, and analyzed by MALDI-MS.

For sequence analysis of the differential peaks, the above resulting tryptic peptides were online injected onto a C-18 reversed-phase nano-column (Discovery BIO Wide pore, Supelco) and analyzed in a continuous acetonitrile gradient. A flow rate of ca. 300 nL/min was used to elute peptides from the reversed-phase nano-column to an electrospray ion source coupled to an ion trap mass spectrometer (Esquire HCT, Bruker Daltonics) for real-time ionization and fragmentation. Single ion monitoring experiments of the selected masses were performed to take advantage of the higher sensitivity into the mass analyzer.

### Immunoblotting

Cell lysis and immunoblotting were as described.<sup>12</sup>

### MMP-13 Activity Assay

MMP-13 activity was assayed by using MMP-13 fluorescence substrates as described.<sup>13</sup>

### Statistical Analysis

Unless otherwise specified, data are expressed as means ± SD, and experiments were performed at least 3 times in duplicate. Whenever comparisons were made with a common control, comparisons were made with analysis of variance followed by Dunnett modification of the *t* test. The level of statistical significance was defined as *P* < 0.05. Error bars represent ± SD.

## Results

### Lack of NOS3 Increases Atherosclerotic Lesion Size in ApoE-Null Mice

We compared atherosclerotic lesions in apoE-null mice and NOS3/apoE—double null mice fed with high-cholesterol diet for 16 weeks. Morphometric analysis of plaque accumulation revealed that lesion sizes were significantly increased (26% larger) in mice lacking NOS3, as detected by eosin and hematoxylin staining of aortic sections. In addition, full-size aortas were longitudinally sectioned and stained with Oil Red O, finding a 66% increase in lipid accumulation in NOS3/apoE—double null mice (Figure 1).

### Lack of NOS3 Increases Macrophage Infiltration in Atherosclerotic Lesions

We collected blood from mice fed with high cholesterol diet for 16 weeks, finding no differences in MOMA-2—positive cells as detected by flow cytometry (Figure 2A). However, immunostaining of aortic sections (Figure 2C), as well as flow cytometry of the same aortas (Figure 2B), revealed a significant increase of macrophage infiltration in mice lacking NOS3.

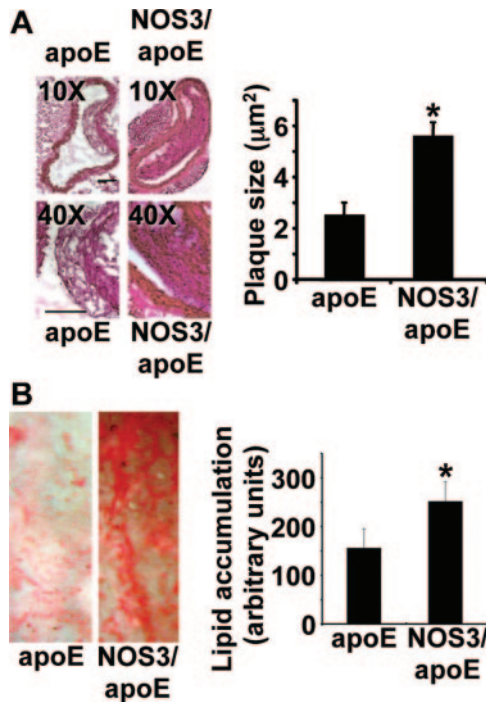


**Figure 1.** Lack of NOS3 increases lesions in mice. A, Aortic sections of mice fed with Western-type diet for 16 weeks, and stained with HE (Scale bars 50 μm). B, Oil Red staining showing lipid deposition on thoracic aortas from the same mice as in A (n=10 mice per group, mean±SD; \*P<0.05 vs NOS3/apoE).

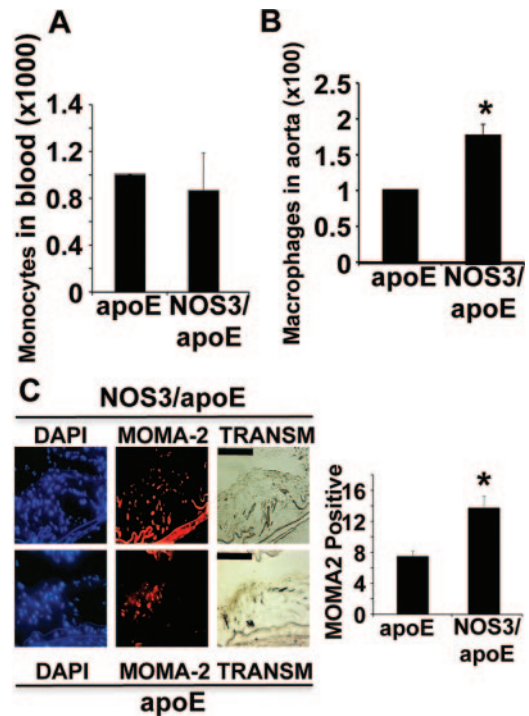


**Figure 2.** Lack of NOS3 increases macrophage infiltration. MOMA-2-positive cells collected from blood (A), or aortic homogenates (B), of mice fed with Western-type diet. C, Confocal microscopy detection of MOMA-2 in aortic rings (Cy3-red, Nuclei-DAPI-blue). TRANSM: Bright field visualization (n=10 mice, mean±SD; \*P<0.05 vs NOS3/apoE). Scale bars, 50 μm.

### Lack of NOS3 Inhibits MMP Expression in Atherosclerosis

We analyzed the expression profile of MMP-2, MMP-9, MMP-12, MT1-MMP, and MMP-13 over time during atherosclerosis, finding no significant differences on MMP-2, MMP-9, MMP-12, and MT1-MMP levels between mice. By contrast, a significant enhancement of MMP-13 was detected in apoE-null mice with respect to mice lacking NOS3, as detected by immunohistochemistry (Figure 3A, left) and by immunoblot with specific antibodies (Figure 3A, right). MMP-13 activity was also increased in the aortas expressing NOS3 (Figure 3B).

### MMP-13 Cleaves ICAM-1 in Aortic Endothelial Cells

The results presented above indicate that lack of endothelial NO increases macrophage infiltration and inhibit MMP-13 production (Figures 2 and 3). Taking into account that lack of NOS3 inhibits MMP-13 in early atherosclerosis, and that adhesion molecules might serve as substrates for MMPs, we postulate that NO may inhibit atherosclerosis at least in part by inducing MMP-13 cleavage of adhesion proteins. In this regard, the levels of chemoattractant protein MCP-13, a recognized substrate of MMP-13,<sup>14</sup> were significantly reduced in NOS3/apoE, compared to apoE-null mice (supplemental Figure I, available online at <http://atvb.ahajournals.org>).

We found no significant differences on ICAM-1, VCAM-1, or PECAM-1 content between mice (data not shown). However, high-cholesterol diet induced a significant

reduction of ICAM-1 levels, as detected by immunohistochemistry and immunoblot (Figure 4A). To determine the involvement of MMP-13 on this effect, we first incubated purified 6XHis tagged ICAM-1 (6XHis-ICAM-1), in the presence or absence of active MMP-13 in a dose-dependent manner, finding that 1 μg MMP-13 was sufficient to cleave ICAM-1 in a 15 minute reaction, as detected by immunoblot with anti ICAM-1 and anti-6XHis antibodies (Figure 4B). A better time course was obtained by reducing the reaction time, finding that MMP-13 cleaved ICAM-1 between 5 and 10 minutes of incubation under these experimental conditions (Figure 4C).

The effect of MMP-13 on cell adhesion was evidenced in COS-7 cells expressing ectopic ICAM-1, finding that incubation with 1 μg MMP-13 induced a significant inhibition of RAW 264.7 cell adhesion to COS-7 cell monolayers (Figure 5A).

To verify the effect of MMP-13 on ICAM-1, we did MALDI-TOF mass spectrometry analysis on ICAM-1 incubated with and without recombinant active MMP-13, finding 2 cleavage sites at positions 61 and 98 of ICAM-1 (Figure 5B). Peaks at m/z 1080.6 and 2993.5 Da correspond to ICAM-1 tryptic peptides spanning sequences highlighted, as determined by sequence analysis of LC-MS (supplemental Figures II and III). Both masses were only present in the nontreated ICAM-1 molecule, but were absent when ICAM-1 was preincubated with MMP-13, suggesting a potential cleavage site by MMP-13 into these sequences. Mass at m/z 4277

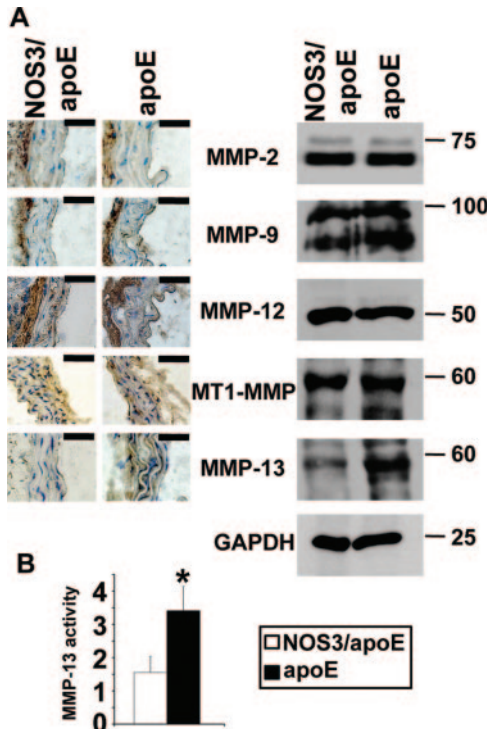


**Figure 3.** Lack of NOS3 inhibits MMP-13 during atherosclerosis. A, Immunohistochemical (left) and immunoblot (right) detection of MMP-2, MMP-9, MMP-12, MT1-MMP, MMP-13, and GAPDH (control) in aortas. Scale bars, 50  $\mu$ m. B, MMP-13 assay represented as increased respect to NOS3/apoE fed with regular diet (NOS3/apoE control) (n=10, mean  $\pm$  SD; \*P<0.05 vs apoE).

Da was only detected in the preincubated sample and matches the gray-boxed sequence. The cleavage site located at G98 locates in a PDGQS moiety showing high homology (indicated with asterisks) with the sequence PQGLS, a reported consensus sequence for cleavage of type II 1-alpha collagen by MMP-13 (Figure 5B bottom). Liquid chromatography coupled to Ion Trap Mass Spectrometry on ICAM-1 was performed to detect peptide sequences as control (supplemental Figures II and III).

These results point to ICAM-1 as a substrate for MMP-13, suggesting a new role of MMP-13 in early atherosclerosis.

### Discussion

We found that lack of NOS3 induces monocyte infiltration, increases lesion size, reduces MMP-13 expression, and preserves endothelial ICAM-1 levels in the aortas of atherosclerotic apoE-null mice. MMP-13 induces ICAM-1 cleavage both in vitro and in vivo, suggesting a molecular way of protection induced by MMP-13 in NOS3-expressing mice.

Endothelial NO inhibits leukocyte-endothelial adhesion,<sup>15</sup> smooth muscle cell migration,<sup>16</sup> and platelet aggregation.<sup>17</sup> However, the mechanisms by which NOS3 could prevent atherosclerosis still remain unclear. Tetrahydrobiopterin (BH4) has been proposed as a candidate to explain this effect. Depending on BH4 availability NOS3 may produce anion superoxide and promote atherosclerosis.<sup>18</sup> In this context, anion superoxide may react with NO

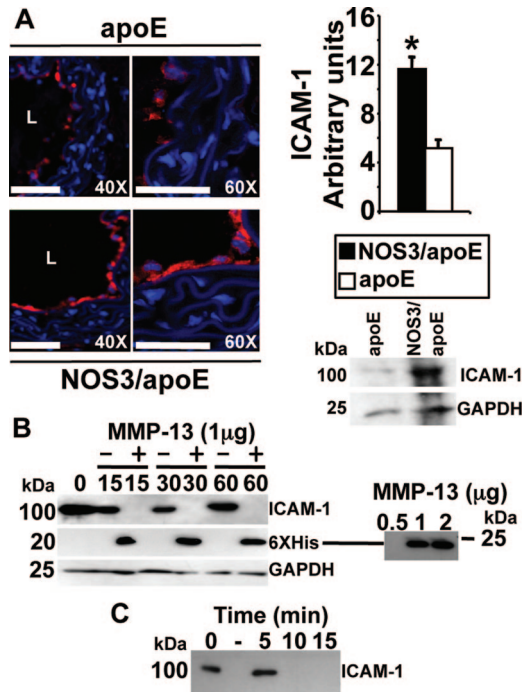


**Figure 4.** MMP-13 induces cleavage of ICAM-1. A, Confocal (left panels, Cy3-red), and immunoblot (lower-right panel) detection of ICAM-1. Scale bars, 50  $\mu$ m. L indicates Lumen. (n=10 aortas, mean  $\pm$  SD; \*P<0.05 vs NOS3/apoE). Time course (B, left) and dose response (B, right, 15 minute-incubation) of 10  $\mu$ g-6XHis-ICAM-1 by MMP-13. (n=3, -: boiled MMP-13).

to produce peroxynitrite, increasing atherosclerotic damage.<sup>18</sup> Interestingly, we found that peroxynitrite induces MMP-13 activation by nitration of tyrosine 338 of the protease.<sup>13</sup> Acute administration of BH4 or sepiapterin, a precursor of BH4, decreases superoxide production and improves endothelial function.<sup>19</sup>

The role of matrix metalloproteinases in atherosclerosis has been proposed.<sup>20</sup> MMP-2, MMP-9, and MMP-12, deficiency are correlated with significant reduction in plaque formation in mouse aortas.<sup>20-23</sup> We previously found that MMP-13 expression is significantly reduced in the aortas of NOS3-null mice, and that NO transcription-

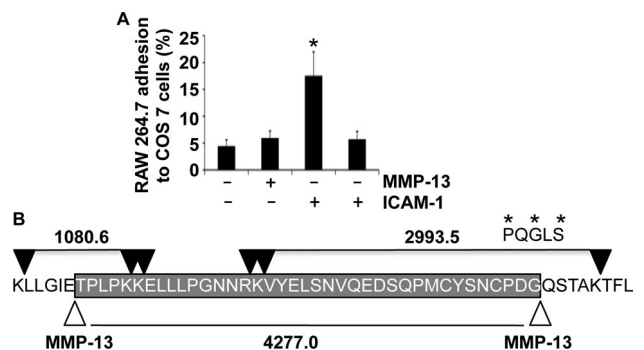


**Figure 5.** MMP-13 cleaves ICAM-1. A, Adhesion of RAW 264.7 cells on COS-7 expressing ectopic ICAM-1 plus 1  $\mu$ g MMP-13. (n=3, mean  $\pm$  SD \*P<0.05 COS-7 ICAM-1+ vs COS-7 ICAM-1+ plus MMP-13). B, MS analysis of ICAM-1 sequence spanning residues 56 to 106 showing tryptic (black triangles) and MMP-13 (white) cleavage sites.

ally regulates MMP-13 expression through the cGMP-PKG pathway in aortic endothelial cells.<sup>9,12</sup> In addition, we also found that NO increases MMP-13 proteolytic activity by nitration of tyrosine residue 338.<sup>13</sup> Here we show that MMP-13 expression is not induced in atherosclerotic NOS3/apoE-null mice, suggesting that NOS3-mediated protection of atherosclerosis may at least be mediated by MMP-13.

Interestingly, Deguchi and coworkers found that MMP-13 deficiency, rather than alterations in lesion size, is correlated with changes in collagen deposition and collagen fibers alignment in atherosclerotic plaques.<sup>20–23</sup> In NOS3/apoE-null mice MMP-13 expression was significantly reduced but not abolished, which may explain the differences in monocyte infiltration and lesion sizes. This apparent contradiction may be explained by the fact that NOS3 may inhibit atherosclerosis by means of several pathways, but also by the fact that knocking down a single MMP may lead to a gain of function of other MMPs. In this regard, it should be interesting to evaluate NOS3 levels in the aortas of MMP-13-null mice. In any case, both works point to MMP-13 as an important antiatherogenic molecule and, in addition to BH4, we propose MMP-13 as another candidate for the NO-mediated prevention of atherosclerosis.

MMPs induce smooth muscle cell and endothelial cell migration, contributing to plaque formation in atherosclerosis.<sup>4,5</sup> However, it has been shown that MMP-9, MT1-MMP, and TACE may also induce proteolysis of adhesion molecules, and therefore may regulate monocyte adhesion and macrophage infiltration.<sup>6,24,25,26</sup> In addition to extracellular matrix components, MMP-13 was found to process more proteins, including prolactin<sup>27</sup> and chemoattractant protein MCP-3.<sup>14</sup> Here we found that MMP-13 also cleaves ICAM-1, both in vivo and in vitro, in a region close to the extracellular N-terminal domain, mapping 2 target sites at positions E61 and G98.

MMP-13 may be considered antiatherogenic because processing of prolactin induces a 16-kDa fragment with strong antiangiogenic properties.<sup>27</sup> On the other hand, atherosclerosis is an inflammatory disease, and MMP-13 may inhibit inflammation by degrading MCP-3.<sup>14</sup> In support of this hypothesis, we found that MMP-13 also cleaves ICAM-1, which may reduce macrophage infiltration as well.

Other MMPs induce proteolytic processing of ICAM-1 releasing full-length soluble ICAM-1.<sup>6,24,26</sup> By contrast, MMP-13 may release a 12-kDa ICAM-1 N-terminal domain. The effect of MMP-13-derived ICAM-1 peptide on atherosclerosis is now under investigation. Taking into account that lack of NOS3 worsens atherosclerosis and inhibits MMP-13 expression, ICAM-1 processing may be considered an additional mechanism for the NOS3 protective effect on this pathology by inhibition of monocyte adhesion.

### Acknowledgments

We thank Dr Francisco Sánchez-Madrid and Dra. Alicia García Arroyo for kindly donation of reagents, and Dr Valentin Fuster for valuable suggestions.

### Sources of Funding

This work was supported by research grant from “Ministerio de Educación y Ciencia” (SAF2007-06025).

### Disclosures

None.

### References

- Glass CK, Witztum JL. Atherosclerosis. the road ahead. *Cell*. 2001;104:503–516.
- Huo Y, Ley K. Adhesion molecules and atherogenesis. *Acta Physiol Scand*. 2001;173:35–43.
- Collins RG, Velji R, Guevara NV, Hicks MJ, Chan L, Beaudet AL. P-Selectin or intercellular adhesion molecule (ICAM)-1 deficiency substantially protects against atherosclerosis in apolipoprotein E-deficient mice. *J Exp Med*. 2000;191:189–194.
- Newby AC. Dual role of matrix metalloproteinases (matrixins) in intimal thickening and atherosclerotic plaque rupture. *Physiol Rev*. 2005;85:1–31.
- Galis ZS, Khatri JJ. Matrix metalloproteinases in vascular remodeling and atherogenesis: the good, the bad, and the ugly. *Circ Res*. 2002;90:251–262.
- Sultan S, Gosling M, Nagase H, Powell JT. Shear stress-induced shedding of soluble intercellular adhesion molecule-1 from saphenous vein endothelium. *FEBS Lett*. 2004;564:161–165.
- Kuhlencordt PJ, Gyurko R, Han F, Scherrer-Crosbie M, Aretz TH, Hajjar R, Picard MH, Huang PL. Accelerated atherosclerosis, aortic aneurysm formation, and ischemic heart disease in apolipoprotein E/endothelial nitric oxide synthase double-knockout mice. *Circulation*. 2001;104:448–454.
- Herman AG, Moncada S. Therapeutic potential of nitric oxide donors in the prevention and treatment of atherosclerosis. *Eur Heart J*. 2005;26:1945–1955.
- Lopez-Rivera E, Lizarbe TR, Martinez-Moreno M, Lopez-Novoa JM, Rodriguez-Barbero A, Rodrigo J, Fernandez AP, Alvarez-Barrientos A, Lamas S, Zaragoza C. Matrix metalloproteinase 13 mediates nitric oxide activation of endothelial cell migration. *Proc Natl Acad Sci U S A*. 2005;102:3685–3690.
- Barreiro O, Yañez-Mo M, Serrador JM, Montoya MC, Vicente-Manzanares M, Tejedor R, Furthmayr H, Sanchez-Madrid F. Dynamic interaction of VCAM-1 and ICAM-1 with moesin and ezrin in a novel endothelial docking structure for adherent leukocytes. *J Cell Biol*. 2002;157:1233–1245.
- Zaragoza C, Lopez-Rivera E, Garcia-Rama C, Saura M, Martinez-Ruiz A, Lizarbe TR, Martin-de-Lara F, Lamas S, Cbfa-1 mediates nitric oxide regulation of MMP-13 in osteoblasts. *J Cell Sci*. 2006;119:1896–1902.
- Zaragoza C, Balbin M, Lopez-Otin C, Lamas S. Nitric oxide regulates matrix metalloproteinase-13 expression and activity in endothelium. *Kidney Int*. 2002;61:804–808.
- Lizarbe TR, Garcia-Rama C, Tarin C, Saura M, Calvo E, Lopez JA, Lopez-Otin C, Folgueras AR, Lamas S, Zaragoza C. Nitric oxide elicits functional MMP-13 protein-tyrosine nitration during wound repair. *FASEB J*. 2008;22:3207–3215.
- McQuibban GA, Gong JH, Wong JP, Wallace JL, Clark-Lewis I, Overall CM. Matrix metalloproteinase processing of monocyte chemoattractant proteins generates CC chemokine receptor antagonists with anti-inflammatory properties in vivo. *Blood*. 2002;100:1160–1167.
- Napoli C, de Nigris F, Williams-Ignarro S, Pignalosa O, Sica V, Ignarro LJ. Nitric oxide and atherosclerosis: an update. *Nitric Oxide*. 2006;15:265–279.
- Kahn AM, Allen JC, Seidel CL, Zhang S. Insulin inhibits migration of vascular smooth muscle cells with inducible nitric oxide synthase. *Hypertension*. 2000;35:303–306.
- Antl M, von Bruhl ML, Eiglsperger C, Werner M, Konrad I, Kocher T, Wilm M, Hofmann F, Massberg S, Schlossmann J. IRAG mediates NO/cGMP-dependent inhibition of platelet aggregation and thrombus formation. *Blood*. 2007;109:552–559.
- Takaya T, Hirata K, Yamashita T, Shinohara M, Sasaki N, Inoue N, Yada T, Goto M, Fukatsu A, Hayashi T, Alp NJ, Channon KM, Yokoyama M, Kawashima S. A specific role for eNOS-derived reactive oxygen species in atherosclerosis progression. *Arterioscler Thromb Vasc Biol*. 2007;27:1632–1637.
- Moens AL, Kass DA. Tetrahydrobiopterin and cardiovascular disease. *Arterioscler Thromb Vasc Biol*. 2006;26:2439–2444.

20. Prescott MF, Sawyer WK, Von Linden-Reed J, Jeune M, Chou M, Caplan SL, Jeng AY. Effect of matrix metalloproteinase inhibition on progression of atherosclerosis and aneurysm in LDL receptor-deficient mice overexpressing MMP-3, MMP-12, and MMP-13 and on restenosis in rats after balloon injury. *Ann N Y Acad Sci*. 1999;878:179–190.
21. Deguchi JO, Aikawa E, Libby P, Vachon JR, Inada M, Krane SM, Whittaker P, Aikawa M. Matrix metalloproteinase-13/collagenase-3 deletion promotes collagen accumulation and organization in mouse atherosclerotic plaques. *Circulation*. 2005;112:2708–2715.
22. Galis ZS, Johnson C, Godin D, Magid R, Shipley JM, Senior RM, Ivan E. Targeted disruption of the matrix metalloproteinase-9 gene impairs smooth muscle cell migration and geometrical arterial remodeling. *Circ Res*. 2002;91:852–859.
23. Kuzuya M, Kanda S, Sasaki T, Tamaya-Mori N, Cheng XW, Itoh T, Itohara S, Iguchi A. Deficiency of gelatinase a suppresses smooth muscle cell invasion and development of experimental intimal hyperplasia. *Circulation*. 2003;108:1375–1381.
24. Fiore E, Fusco C, Romero P, Stamenkovic I. Matrix metalloproteinase 9 (MMP-9/gelatinase B) proteolytically cleaves ICAM-1 and participates in tumor cell resistance to natural killer cell-mediated cytotoxicity. *Oncogene*. 2002;21:5213–5223.
25. Sithu SD, English WR, Olson P, Krubasik D, Baker AH, Murphy G, D'Souza SE. Membrane-type 1-matrix metalloproteinase regulates intracellular adhesion molecule-1 (ICAM-1)-mediated monocyte transmigration. *J Biol Chem*. 2007;282:25010–25019.
26. Tsakadze NL, Sithu SD, Sen U, English WR, Murphy G, D'Souza SE. Tumor necrosis factor-alpha-converting enzyme (TACE/ADAM-17) mediates the ectodomain cleavage of intercellular adhesion molecule-1 (ICAM-1). *J Biol Chem*. 2006;281:3157–3164.
27. Macotela Y, Aguilar MB, Guzman-Morales J, Rivera JC, Zermeno C, Lopez-Barrera F, Nava G, Lavalle C, Martinez de la Escalera G, Clapp C. Matrix metalloproteases from chondrocytes generate an antiangiogenic 16 kDa prolactin. *J Cell Sci*. 2006;119:1790–1800.